Available online www.ejaet.com

European Journal of Advances in Engineering and Technology, 2020, 7(10):40-46

Research Article ISSN: 2394 - 658X

Fatigue Strength of Self-piercing Riveted Joints in Lap-shear Specimens of Dissimilar Magnesium Alloy Sheets

W.T. Hwang[1], J.J. Han[1] and H.K. Kim[2]

[1]Automotive Dept.Graduate School, Seoul National Univ. of Sci. Tech., Republic of Korea
[2]Dept. of Mechanical & Automotive Eng. Seoul National Univ. of Sci. Tech., Republic of Korea
kimhk@seoultech.ac.kr

ABSTRACT

As an alternative to resistance spot-welding, SPR joining has been considered to join dissimilar material sheets in the automotive industry. In this study, the static and fatigue strengths of tensile-shear specimens with a SPR joint of AZ31 magnesium alloy and Al5052 aluminum alloy sheets were evaluated. In addition, finite element method (FEM) analyses were carried out on these specimens to estimate their stress distributions. The static strength of the specimens was 3,315N. Assuming a fatigue limit of 10^6 cycles, the fatigue ratio was 26%. From SEM observations of the fatigue specimen surfaces, fatigue cracks were found to initiate at a certain point located a few millimeters from the center of the rivet, at which the upper and lower sheets were in contact. Cracks propagated through the upper sheet thickness and simultaneously propagated laterally toward the direction of the load. A structural analysis demonstrated that the locations at which the maximum value of the von-Mises and maximum principal stresses occur are similar to each other. However, the locations at which the maximum values of these stresses arise differ from the fatigue crack initiation sites.

Key words: Self-piercing riveting, Magnesium alloy, Fatigue strength, Monotonic strength

---

INTRODUCTION

Automotive manufactures must reduce vehicle emissions to respect new environmental regulation laws. As one way to cope with this matter, they are concerned about vehicle weight reductions. The use of magnesium alloys is considered to be a variable means of realizing lighter vehicle bodies. Magnesium alloys have superior specific strength and specific modulus as well as excellent vibration-damping capacities. Therefore, the use of magnesium alloys in automobile components is increasing [1].

Resistance spot-welding is mainly used to join steel panels in vehicle bodies. However, it is difficult to apply this welding technique to join steel and other material sheets, such as magnesium, aluminum, titanium and composite sheets, due to differences in the melting temperatures and electrical resistances of the two facing materials in these cases. Recently, many joining techniques, such as self-piercing riveting [2], spot friction welding [3], and clinched joining [4], have been considered to join these dissimilar material sheets in the automotive industry.

As an alternative to resistance spot-welding, SPR joining is a cold-forming process capable of fastening two or more sheets by driving a semi-tubular rivet, as shown in Fig. 1. During SPR joining, a mechanical interlock is formed by the rivet when it pierces the upper sheet and flares in the lower sheet under the guidance of the die geometry [2]. The SPR method has the advantage of being able to combine two different sheets with plastic deformation. Thus, no additional materials other than rivets are required, and the static and fatigue strength are excellent. Moreover, this method is environmentally friendly because no harmful substances, such as fumes, are generated [2].

A limited number of studies have focused on SPR joining for magnesium alloy sheets [5-10]. For example, Wang et al. studied the conditions of SPR joints of AZ31 magnesium alloy sheets [5]. They reported that defects were found in the lower sheet when using the SPR joining method at room temperature. Thus, they evaluated preheating temperatures and strain rates of AZ31 magnesium alloy sheets by applying the Zener-Hollomon parameter. As a result, the appropriate preheating temperature range for SPR joining without defects was found to be 180 to 200^{o}C, and the strain rate was also confirmed to be4 s^{-1}. Durandet et al. proposed laser-assisted self-piercing riveting (LSPR) for AZ31 magnesium alloy sheets [6]. They demonstrated that dynamic recrystallization is limited during SPR joining at room temperature, and

cracks are not observed if the AZ31 magnesium alloy is preheated to a temperature greater than 200^{o}Cusing a laser. It was also reported that the strength of the SPR joints was found to be affected by the length and hardness of the rivets, a finding which allowed the LSPR method to meet various strength requirements. Recently, Kang et al. investigated the monotonic and fatigue strengths of SPR joints of magnesium alloys and steel sheets, which were evaluated using cross-shaped specimens at loading angles of 0^{o}, 45^{o}, and 90^{o} [7]. The fatigue ratios (= fatigue endurance limit/static strength) at the loading angles of 0^{o}, 45^{o}, and 90^{o} were reported to be 22%, 13%, and 9%, respectively. They argued that the fatigue lifetimes of SPR joints could be evaluated most appropriately by considering the maximum principal stress.

In particular, there are few studies of the fatigue strength of SPR joints of dissimilar magnesium alloy sheets. Therefore, in this study, the monotonic strength and fatigue strength of tensile-shear specimen with a SPR joint of AZ31 magnesium alloy and Al5052 aluminum alloy sheets were evaluated. In addition, finite element method (FEM) analyses were carried out on the tensile-shear specimens to estimate the stress distributions of the specimens. The fracture modes and surfaces of the specimens were also observed by means of SEM.

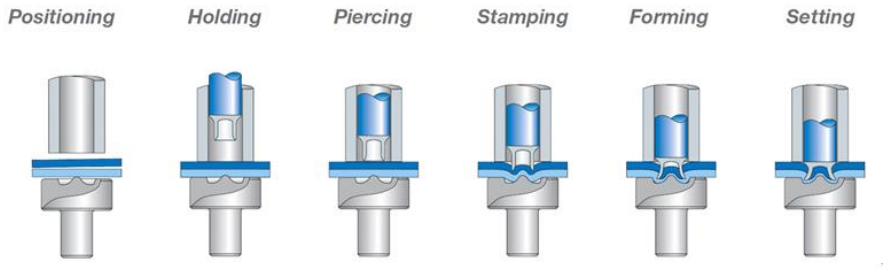

Fig. 1 Schematic representation of the SPR process

EXPERIMENTAL

Specimen materials and preparation

In this study, Al5052 aluminum alloy and AZ31 magnesium alloy were used to produce the SPR joint specimen. Table 1 summarizes the tensile properties of the Al5052 aluminum alloy and AZ31 magnesium alloy as obtained through tensile tests. It is common to install relatively high-strength or thicker sheet materials as the lower sheet for SPR joining. However, in this study, if magnesium alloy sheet, which has greater strength, is placed as the lower sheet, the magnesium sheet fractures owing to its low formability when the tail of the rivet partially pierces the lower magnesium sheet. Therefore, in this study, the relatively ductile Al5052 aluminum sheet is placed as the lower sheet and the relatively brittle AZ31 magnesium alloy sheet is placed as the upper sheet for the SPR joint specimens. Tensile-shear specimen geometry was used to evaluate the static and fatigue strengths of the SPR joints, as shown in Fig. 2.

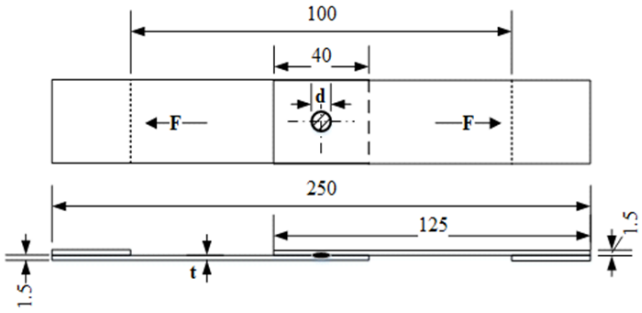

Fig. 2 Dimensions of the tensile-shear specimen

Table -1 Tensile properties of the AZ31 Magnesium alloy and Al5052

Material	σ_u (MPa)	σ_y (MPa)	Elongation (%)
AZ31	277.7	146.9	17
Al5052	216.1	162	12

Static and Fatigue Tests

To evaluate the static and fatigue strengths of the SPR joints, a servo hydraulic universal testing machine (Instron 8516) was used. The diameter and length of the rivet shank used in this study are both 5.3 mm, and the thicknesses of the sheets of AZ31 magnesium alloy and Al5052 aluminum alloy are 1.5 mm. For SPR joints, the joint strength is determined by the shape of the rivet, the thickness of the sheet, the piercing direction of the joint, and the punching force. Therefore,

with the given die shape, sheet thickness (= 1.5mm) and direction of piercing (upper magnesium sheet - lower aluminum sheet), SPR joints were prepared with various punching forces to determine the optimum joint strength. Fatigue testing was performed with a sine wave form and at a load ratio ($R = P_{min} / P_{max}$) of 0.1.

Structural Analysis Modeling

The cross-section of the SPR joint specimen with the optimum punching force (= 32kN) is shown in Fig. 3. Three-dimensional finite element modeling was utilized with the ProE and HyperMesh programs. The three-dimensional model for the SPR joint is shown in Fig. 4, and the three-dimensional finite element analysis model for the specimen including this joint is shown in Fig. 4. An eight-node hexahedral element (C3D8R) was used for modeling, and the model in Fig. 5 consists of 223,521 nodes and 209,452 elements. The contact pair function is used to model the contact surfaces. The coefficient of friction between the materials was determined experimentally. The coefficient of friction between the magnesium alloy and the steel rivets was 0.374, and the coefficient between the magnesium and the aluminum sheet was 0.25. The finite element analysis was conducted using the ABAQUS solver.

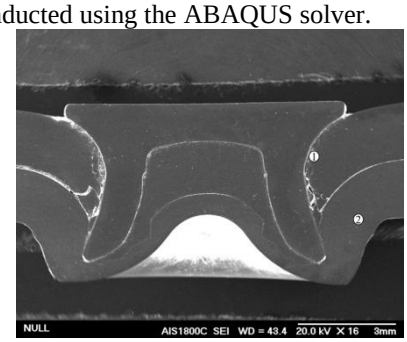

Fig. 3 Cross-section from the center of the SPR joints

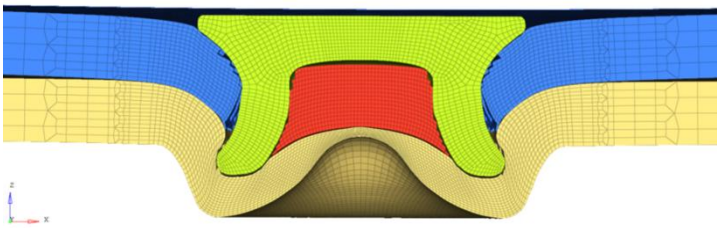

Fig. 4 Cross-section view of the SPR joint in the FEA model

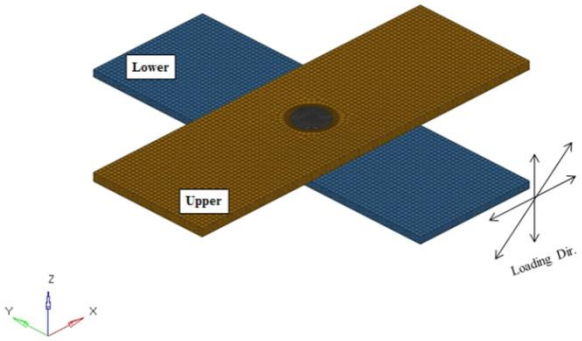

Fig. 5 3-D FEA model of the SPR the joint

EXPERIMENTAL RESULTS AND DISCUSSION

Optimum Punching Force of the SPR Joining

The punching force depends on the joining behavior when two dissimilar sheets are joined through SPR joining. Insufficient punching force prevents the rivet head from coming fully into contact with the top of the upper sheet. On the other hand, if the punching force is excessive, the rivet will cause excessive plastic deformation of the lower sheet, causing the upper and lower sheets to bend and the rivet head to sink into the upper sheet. Here, the tensile-shear specimens were prepared with various punching forces to verify the optimum punching force that offers the best joint strength. Fig. 6 presents the maximum joint strengths for tensile-shear specimens produced with various punching forces. With a rivet properly punched without excessive plastic deformation, the punching force with the highest joint strength was found to be 32kN, as shown in Fig. 6. Therefore, cross-shaped specimens and tensile-shear specimens were produced with a punch load of 32kN to evaluate the static and fatigue strengths.

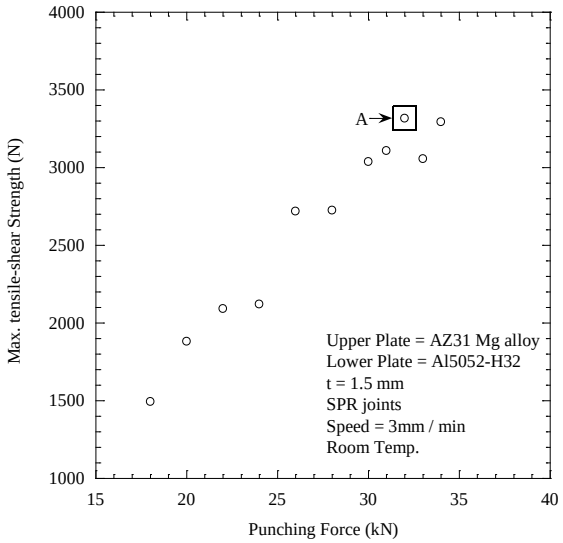

Fig. 6 Punching force against the maximum monotonic strength for the tensile-shear specimen with a combination of an upper AZ31 alloy sheet and a lower Al5052 alloy sheet

Static and fatigue strength of SPR joints

Fig. 7 shows the static test results for the SPR joint specimen. This figure shows that the static load of the specimen peaked at about 3,315 N, causing partial separation of the upper and lower sheets of the joint from the maximum load, with the specimen ultimately fracturing. Fatigue tests were also carried out on the SPR joint specimen. Fig. 8 shows the load amplitudes and fatigue lifetimes. From Fig. 8, the relationship between the load amplitude and the number of cycles was found to be $P_{amp} = 4{,}696.0N_f^{-0.124}$. Assuming a fatigue endurance limit of 10^6 cycles, the load amplitude corresponding to the fatigue limit of the SPR joint is 847N, which is approximately 26% of the static strength (P = 3,315 N).

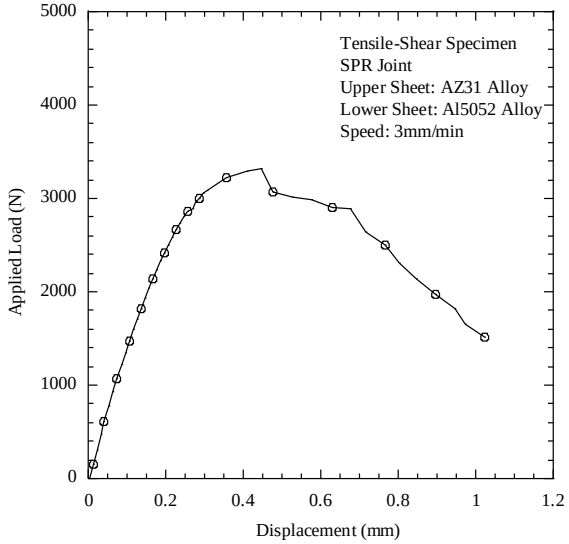

Fig. 7 Static load versus the displacement curve of the tensile-shear SPR joint specimen

Fatigue Failure Modes

For the fatigue test specimens, fatigue crack initiation generally occurred near the rivet on the upper magnesium sheet and propagated across the upper sheet in all tests. The fatigue-fractured surfaces and wear scars at the interfaces between the magnesium sheet and the rivet were investigated using a scanning electron microscope (SEM, Model TESCAN VEGA3).Fig. 9 shows an example of a fracture surface of a fatigued specimen with a load amplitude (P_{amp}) of 1,000N and the fatigue life of 244,825 cycles. For this specimen, as shown in Fig. 9(e), crack initiation occurred at a point not less than 1 mm from the rivet head end on the upper magnesium sheet and propagated normal to the direction of the load. Fig. 9(a) shows the surface of the upper sheet viewed from the direction of the arrow in Fig. 9(e). In order to determine the crack initiation location and the propagation direction on the test specimen, the three areas indicated by the red boxes in Fig. 9(a) were magnified by SEM, as shown in Figs. 9(b), 9(c), and 9(d). Visually, some parts of the fatigue fractured

surfaces show fretting wear due to repeated contact with the separated fracture faces. In addition, the white particles on the fatigue-fractured surfaces are magnesium oxides, which are believed to have been caused friction heat due to repeated contact between separated fracture surfaces. It is believed that crack initiation occurred at the lower part of the magnesium sheet in Fig. 9(c), where the magnesium upper sheet and the aluminum lower sheet meet at a point more than 1 mm from the head end of the rivet. This crack propagates in the direction of the arrow shown in this figure. Fig. 9(b) is a magnified image of the left square area shown in Fig. 9(a). It is believed that the initiated crack propagated in the direction of the upper section of the upper sheet, as shown in Fig. 9(b). Fig. 9(d) is a magnification of the right square area shown in Fig. 9(a). The initiated another crack is thought to have propagated in the direction of the upper surface of the upper sheet, as indicated by the direction of the arrow in Fig. 9(d). Hence, it is deemed that the crack initiated at a certain point approximately 5 mm from the center of the rivet, at which the upper and lower sheets were in contact, propagated through the upper sheet thickness, and simultaneously propagated laterally to the direction of the load. Most fatigue specimens exhibit a similar fatigue fracture pattern.

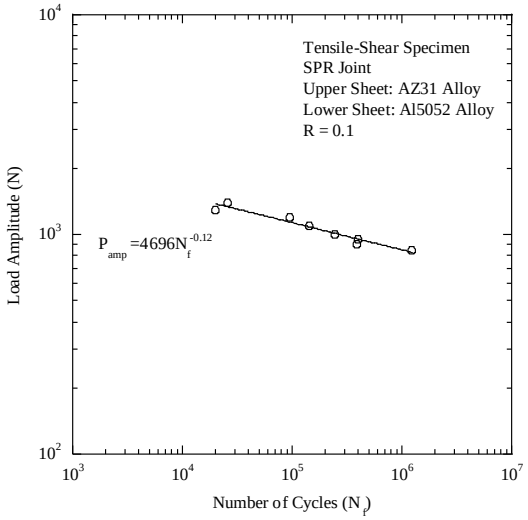

Fig. 8 Load amplitude against the number of cycles plot for the SPR joints

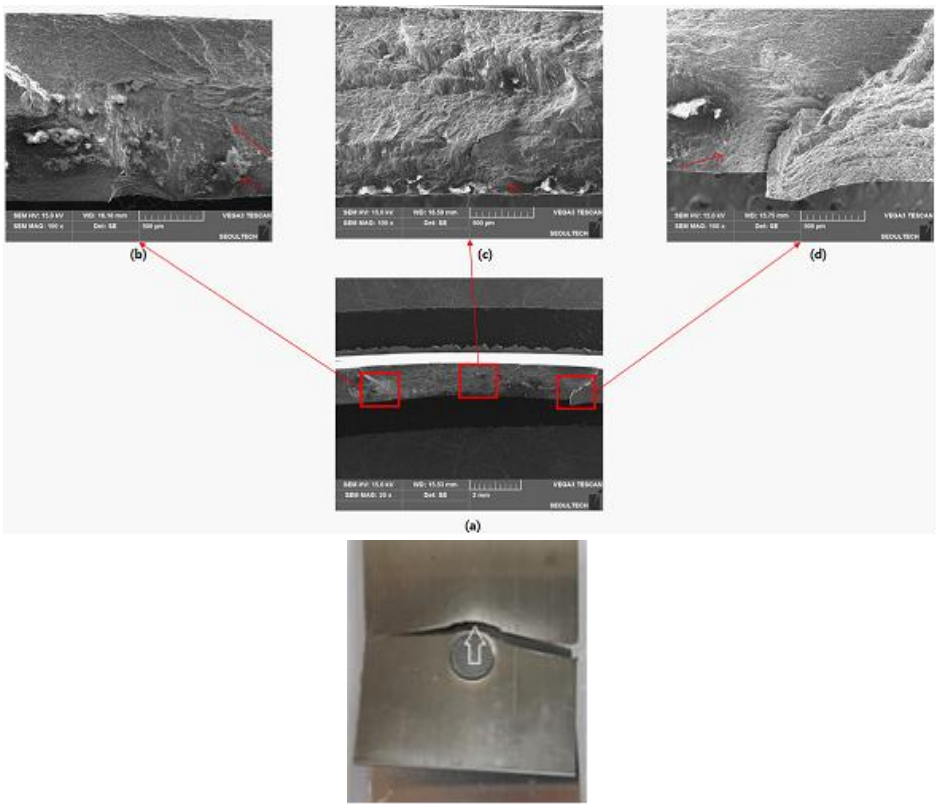

Fig. 9 Fatigue fracture surfaces of the specimen under P_{amp} = 1000 N

Structural Analysis Results

A finite element analysis was conducted on a tensile-shear specimen with a SPR joint. Typically, the stress is more concentrated on the lower sheet when a load is applied to a SPR joint. However, as can be observed in Fig. 9, a fatigue fracture occurred in the upper magnesium alloy sheet, a material of lower strength. Therefore, the structural analysis results are displayed for the upper sheet. Table 3 summarizes the analysis results, showing the maximum values of the von-Mises and maximum principal stresses, their locations, and the location of the crack.

Fig. 10 presents the stress distribution of the SPR joint when a maximum load (P_{max}) of 1,891N is applied with a load amplitude of 851 N at R = 0.1 corresponding to a fatigue life of 10^6 cycles. The direction of the load is the condition in which the tensile force is applied in the right direction on the upper sheet. Fig. 10(a) presents the von-Mises stress distribution, confirming that maximum stress of 230.8MPa occurred on the upper sheet concave surfaces in contact with the lower sheet. Fig. 10(b) shows the maximum principal stress distribution. The maximum value of 187.8MPa was found on the upper sheet concave surfaces in contact with the lower sheet. This location with the maximum value is similar to that of the von-Mises stress. As described with reference to the location of crack initiation, as shown in Fig. 9, the point of crack initiation was on the upper sheet approximately 1 mm from the head end of the rivet, the point of contact with the lower sheet. The location at which the maximum value of the maximum principal or von-Mises stress distribution in Fig. 10 occurs is left from the center of the rivet. However, the location at which the fatigue crack actually initiated was on the right side in these figures, in contrast to the maximum stress locations of the two stress parameters.

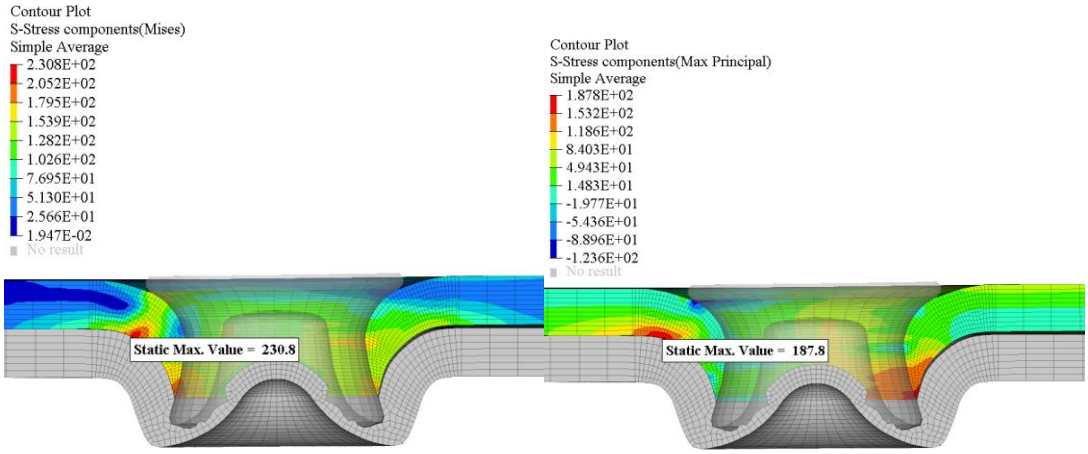

(a) (b)

Fig. 10(a) Von-Mises and (b) maximum principal stress distributions of the SPR joints under P = 1891 N

CONCLUSION

In this study, static and fatigue strengths were evaluated for a tensile-shear specimen of aluminum Al5052 alloy and magnesium AZ31 magnesium alloy sheets. Static tests showed that the maximum static strength was 3,315N. Assuming a fatigue limit of 106 cycles, fatigue endurance limits were found to be 847N. Therefore, the fatigue ratio is 26%. A fatigue crack initiated a few millimeters from the center of the rivet, at the point where the upper and lower sheets were in contact. It then propagated through the upper sheet thickness, while simultaneously propagating laterally toward the direction of the load. As structural analysis found that, the locations at which the maximum value of the von-Mises and maximum principal stresses occur are similar to each other, though these values differed from that where the fatigue crack initiated.

Acknowledgements

This study was financially supported by Seoul National University of Science & Technology.

REFERENCES

[1]. S Logan, A Kizyma, C Patterson, and S Rama, Lightweight magnesium intensive body structure,*SAE Technical Papers*, 2006, 01-0523.

[2]. X He, I Pearson, and K Young, Self-pierce riveting for sheet materials: State of the art,*Journal of Materials Processing Technology*,2008, 199, 27-36.

[3]. E Fereiduni, M Movahedi, and AH Kokabi, Aluminum/steel joints made by an alternative friction stir spot welding process, *Journal of Materials Processing Technology*, 2015, 224, 1-10.

[4]. JB Kim and HK Kim, Fatigue behaviour of clinched joints in a steel sheet, *Fatigue and Fracture of Engineering Materials and Structures*, 2015, 38, 661-672.

[5]. JW Wang, ZX Liu, Y Shang, AL Liu, MX Wang, RN Sun, and P.C. Wang, Self-piercing riveting of wrought magnesium AZ31 sheets, *Journal of Manufacturing Science and Engineering*, 2011, 133(3), 031009.

[6]. Y Durandet, R Deam, A Beer, W Song, and S Blacket, Laser assisted self-pierce riveting of AZ31 magnesium alloy strips,*Materials and Design*,2010, 31(l1), S13-S16.
[7]. SH Kang, DW Han, and HK Kim, Fatigue strength evaluation of self-piercing riveted joints of AZ31 Mg alloy and cold-rolled steel sheet, *Journal of Magnesium and Alloys*, 2020, 8, 241-251.
[8]. Y Miyashita, YC Teowa, T Karasawaa, N Aoyagib, Y Otsukaa, and Y Mutoha, Strength of adhesive aided SPR joint for AM50 magnesium alloy sheets, *Procedia Engineering*,2011, 10, 2532-2537.
[9]. EL Silva, D Hoche, AC Bouali, M Serdechnova, RL Sesenes, CS Scholz, and ML Zheludkevich, Digital modeling of the galvanic corrosion behaviour of a self-piecing riveted AZ31-AA5083 hybrid joint, *Materials Science and Engineering Technology*,2017, 48(6), 529-545.
[10]. V Upadhyay, X Qi, N Wilson, D Battocchi, G Bierwagen, J Forsmark, and R McCune, Electrochemical characterization of coated self-piercing rivets for magnesium applications, *SAE International Journal of Materials and Manufacturing*,2016,9(1), 187-198.